

## Low Core Loss of a bcc Fe<sub>86</sub>Zr<sub>7</sub>B<sub>6</sub>Cu<sub>1</sub> Alloy with Nanoscale Grain Size

著者	Makino Akihiro, Suzuki Kiyonori, Inoue Akihisa, Masumoto Tsuyoshi
journal or publication title	Materials Transactions, JIM
volume	32
number	6
page range	551-556
year	1991
URL	<a href="http://hdl.handle.net/10097/52219">http://hdl.handle.net/10097/52219</a>

# Low Core Loss of a bcc Fe<sub>86</sub>Zr<sub>7</sub>B<sub>6</sub>Cu<sub>1</sub> Alloy with Nanoscale Grain Size

Akihiro Makino\*\*, Kiyonori Suzuki\*†, Akihisa Inoue\*  
and Tsuyoshi Masumoto\*

We have investigated the possible applications potential of a newly developed bcc-nanocrystalline Fe<sub>86</sub>Zr<sub>7</sub>B<sub>6</sub>Cu<sub>1</sub> alloy by determining the core loss, permeability  $\mu_e$ , and magnetization  $B_{800}$  (at a field 800 kA/m). The above parameters have been studied as a function of annealing temperature  $T_a$  of the as-quenched amorphous alloy, maximum induction  $B_m$ , and frequency (up to 100 kHz). On transformation to the bcc-nanocrystalline state at 873 K with a 10 nm grain size, maximum values of  $\mu_e=41000$  and  $B_{800}=1.52$  T are obtained. The determined core loss is found to achieve a minimum value of 66 mW/kg at 1 T, 50 Hz. This value is considerably smaller (45 and 95% respectively) than those reported for the amorphous Fe<sub>78</sub>Si<sub>9</sub>B<sub>13</sub> and bcc Fe-3.5%Si alloys now in use as transformer core materials. The observed  $B_m$  and frequency dependences of the loss values for our new Fe-Zr-B-Cu alloy are consistently found to be superior as well. Thus, the bcc-nanocrystalline Fe-Zr-B-Cu alloy is quite promising for practical use as a core material in various transformers with the advantage of high  $B_{800}$ , high  $\mu_e$  and low core loss.

(Received January 7, 1991)

**Keywords:** bcc-nanocrystalline alloy, nanoscale grain size, iron-zirconium-boron system, soft magnetic property, core loss, permeability, saturation magnetization, electrical resistivity, crystallization

## I. Introduction

The development of magnetic materials exhibiting high saturation magnetization and good soft magnetic characteristics continues to be in demand for the emerging generation of electric-magnetic devices. It is generally known<sup>(1)</sup> that some amorphous Fe- and Co-based alloys exhibit these requirements as good soft magnetic properties. However, the coexistence of good soft magnetic properties and high saturation magnetization is rather difficult for amorphous alloys because the dissolution of solute elements needed for amorphization usually leads to a decrease of saturation magnetization.

It has been reported<sup>(2)(3)</sup> that soft magnetic properties of Fe-based amorphous ribbons can be significantly improved by precipitating fine sub-micron size crystalline particles with a long time-annealing at temperatures below that for spontaneous crystallization. Recently, by controlled crystallization of amorphous Fe-Si-B-Nb-Cu alloys into a bcc structure with a fine grain size of about 10 nm, good soft magnetic properties combined with a rather high saturation magnetization ( $B_s$ ) of about 1.3 T have been obtained<sup>(4)</sup>. Similar properties with  $B_s$  of 1.5 to 1.6 T have also been obtained for Fe-M-C (M=V, Nb or Ta) thin films consisting of  $\alpha$ -Fe and MC carbides produced by crystallization of their vapor-deposited amorphous phases<sup>(5)</sup>. These results suggest that the use of an amorphous phase as a precursor to obtain ultrafine

crystalline phases is useful to achieve good soft magnetic properties with high saturation magnetization.

More recently, the present authors have examined systematically the relation between crystallization-induced microstructure and magnetic properties for Fe-Zr-B and Fe-Hf-B amorphous alloys. These alloys were chosen because an amorphization by melt spinning has been achieved<sup>(6)(7)</sup> with the highest possible Fe concentration range. As a result, we reported<sup>(8)(9)</sup> that a mostly single bcc phase with nanoscale grain size is obtained in a wide annealing temperature range which exhibits a high permeability of about 15000 as well as a high  $B_s$  of 1.7 T. The high  $B_s$  value and good soft magnetic properties of the bcc Fe-Zr-B alloy allow us to expect that the alloy can be used as a core material in electric power transformers. In order to ascertain the subsequent progress of the newly developed bcc Fe-Zr-B alloy with nanoscale grain size, it is essential to learn about core losses as a function of maximum induction field and frequency. In this paper we present our studies of the change in core losses with annealing temperature for amorphous Fe<sub>86</sub>Zr<sub>7</sub>B<sub>6</sub>Cu<sub>1</sub> alloy. In addition, the induction field and frequency dependences of the minimum core loss obtained at optimum  $T_a$  are also given, with those of commercial amorphous Fe<sub>78</sub>Si<sub>9</sub>B<sub>13</sub> and bcc Fe-3.5 mass%Si alloys. A comparison of our data with those of amorphous Fe<sub>78</sub>Si<sub>9</sub>B<sub>13</sub> and bcc Fe-3.5%Si shows that nanocrystallized Fe-Zr-B-Cu alloys are most promising as core materials in electric power transformers.

## II. Experimental Procedure

A quaternary alloy with composition Fe<sub>86</sub>Zr<sub>7</sub>B<sub>6</sub>Cu<sub>1</sub> was chosen in the present study because it possessed high permeability and relatively large glass-forming capacity

\* Institute for Materials Research, Tohoku University, Sendai 980, Japan.

\*\* Research and Development, Alps Electric Co. Ltd., Nagaoka 940, Japan.

† On leave from Research and Development, Alps Electric Co. Ltd., Nagaoka 940, Japan.

in Fe–Zr–B ternary and Fe–Zr–B–M (M=transition metal) quaternary systems<sup>(9)</sup>. The Fe–Zr–B–Cu alloy ingot was produced by arc melting mixtures of pure Fe (99.9 mass%), Zr (99.5 mass%) and Cu (99.9 mass%) metals and pure B (99.8 mass%) crystal in an argon atmosphere. The subscripts are assumed to be those of the unalloyed pure elements since the difference between nominal and chemically analyzed compositions was less than 0.8 mass% Zr and 0.1 mass% B. Rapidly solidified ribbons with a cross section of about  $0.021 \times 12.5 \text{ mm}^2$  were produced in an argon atmosphere by a single-roller melt spinning method. The copper roller with a diameter of about 250 mm was rotated at a constant circumferential speed of 46 m/s. The ejecting pressure of the molten alloy was 34 kPa. The as-quenched sample was annealed for 3.6 ks at various temperatures ranging from 573 to 973 K in an evacuated state. The heating and cooling rates in the annealing treatment are controlled to be 0.17 K/s. The identification method of as-quenched and annealed structures is described in Ref. (9). In addition, commercial non-oriented bcc Fe–3.5 mass%Si (subjected to an optimum annealing treatment at 993 K) and Fe<sub>78</sub>Si<sub>9</sub>B<sub>13</sub> amorphous alloy (METGLAS 2605S2) were used for comparison.

Magnetization under an applied field of 800 kA/m ( $B_{800}$ ) was measured at room temperature with a vibrating sample magnetometer. Coercive force ( $H_c$ ) under 800 A/m and effective permeability ( $\mu_e$ ) in the frequency range of 1 to  $10^2$  kHz under 0.8 A/m were evaluated at room temperature with a DC B–H loop tracer and a transformer-type method, respectively. The sample used in the transformer-type method had a ring shape with the outer and inner diameters of 10 and 6 mm, respectively. The ring sample was prepared by mechanical punching. The samples with the same shape were also prepared by mechanical punching for the Fe–Si–B amorphous ribbon and by chemical etching for the Fe–Si sheet. The core loss was measured with a U function meter using the ring-shape samples at room temperature. Electrical resistivity was measured at room temperature by a DC four-probe technique. The density used to evaluate the  $B_s$  value was measured by the Archimedian method using tetra-bromoethane.

### III. Results and Discussion

The crystallization behavior of an amorphous Fe<sub>86</sub>Zr<sub>7</sub>B<sub>6</sub>Cu<sub>1</sub> alloy was initially examined in order to obtain a mostly single bcc phase with a nanoscale grain size. Figure 1 shows the DTA curve of an amorphous Fe<sub>86</sub>Zr<sub>7</sub>B<sub>6</sub>Cu<sub>1</sub> alloy heated at a scanning rate of 0.17 K/s. Two exothermic peaks with high and low intensities are seen in the range of 792 to 833 K and 998 to 1016 K, indicating that the crystallization is complete through two stages. As shown in Ref. (9), the high intensity peak at the lower temperature side is due to the transition of amorphous to bcc phase and the low intensity peak at the higher temperature side due to the transition of bcc to  $\alpha$ -Fe + Fe<sub>3</sub>(Zr, B) + Fe<sub>2</sub>(Zr, B) phases. The samples used for

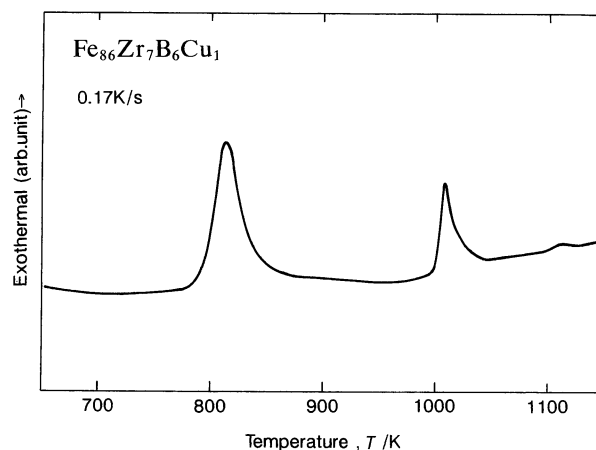


Fig. 1 Differential thermal analysis (DTA) curve of an amorphous Fe<sub>86</sub>Zr<sub>7</sub>B<sub>6</sub>Cu<sub>1</sub> alloy.

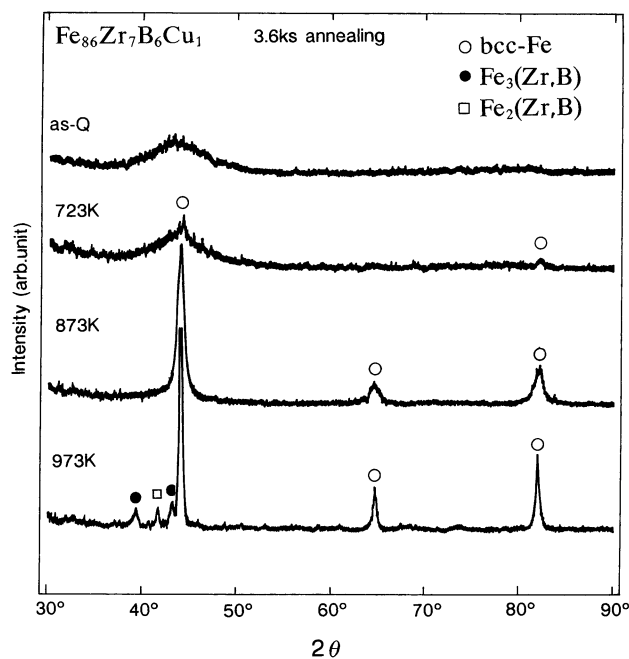


Fig. 2 X-ray diffraction patterns of an amorphous Fe<sub>86</sub>Zr<sub>7</sub>B<sub>6</sub>Cu<sub>1</sub> alloy in an as-quenched state and annealed at 723 to 973 K.

the measurement of magnetic properties were subjected to the isochronal annealing for 3.6 ks as shown later. Accordingly, the annealing temperature range leading to the mostly single bcc phase was examined in the isochronal treatment. Figure 2 shows the change in the X-ray diffraction pattern with annealing temperature ( $T_a$ ). The transition of amorphous to bcc phase begins to occur at 723 K and is almost completed at 773 K. The bcc phase remains unchanged in the wide temperature range of 773 to 923 K. The further increase of  $T_a$  results in a mixed structure of  $\alpha$ -Fe, Fe<sub>3</sub>(Zr, B) and Fe<sub>2</sub>(Zr, B). The lattice parameter ( $a_0$ ) of the bcc phase is measured to be 0.2870 nm after annealing for 3.6 ks at 873 K. The  $a_0$  value is slightly larger than that (0.28664 nm) for pure  $\alpha$ -Fe<sup>(10)</sup>, indicating that the bcc phase contains the solute elements. The  $a_0$  value of the nonequilibrium bcc phase produced by melt spin-

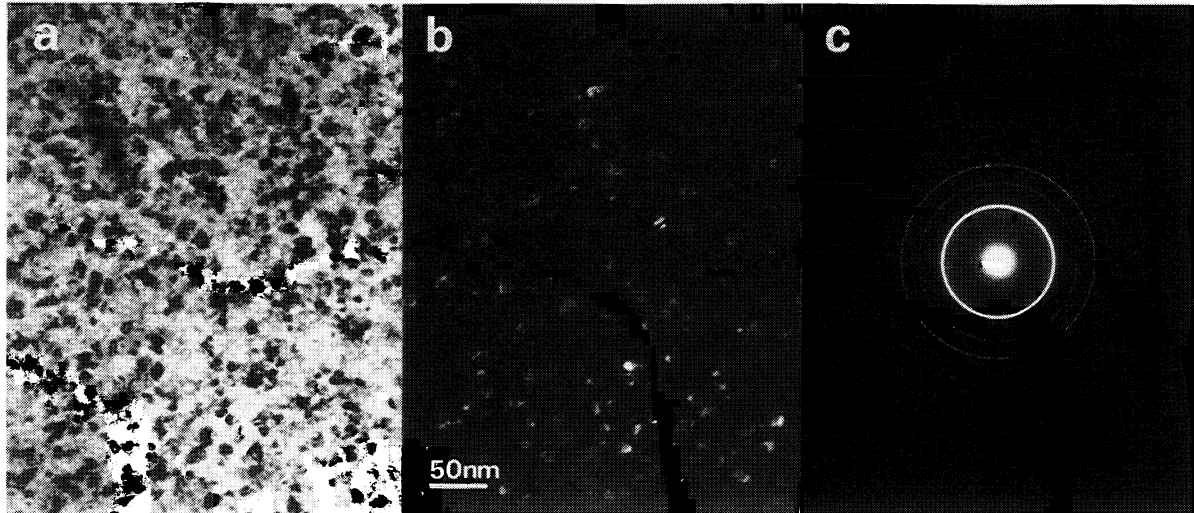


Fig. 3 Bright- and dark-field electron micrographs of an amorphous  $\text{Fe}_{86}\text{Zr}_7\text{B}_6\text{Cu}_1$  alloy annealed for 3.6 ks at 873 K. The dark-field micrograph was taken from the (110) reflection ring of the bcc phase.

ning, vapor deposition and mechanical alloying increases by the dissolution of Zr, *e.g.*, about 0.2884 nm for  $\text{Fe}_{93}\text{Zr}_7$ <sup>(11)</sup>. On the other hand, the dissolution of B causes a decrease in  $a_0$  at a rate of 0.0002 to 0.0003 nm per one atomic percent<sup>(12)</sup>. Accordingly, the smaller  $a_0$  value of the present bcc  $\text{Fe}_{86}\text{Zr}_7\text{B}_6\text{Cu}_1$  alloy in comparison with that<sup>(11)</sup> for the bcc  $\text{Fe}_{93}\text{Zr}_7$  alloy seems to result from the dissolution of B. As an example, Fig. 3 shows bright- and dark-field electron micrographs and a selected area diffraction pattern of the  $\text{Fe}_{86}\text{Zr}_7\text{B}_6\text{Cu}_1$  alloy annealed for 3.6 ks at 873 K. The sample consists of a bcc structure with a homogeneous grain size of about 10 nm even at 873 K which is located at the highest temperature side in the bcc phase field. Consequently, the Fe-Zr-B-Cu alloy is concluded to be an appropriate composition to obtain a bcc structure with nanoscale-grain size by annealing the amorphous precursor.

Figure 4 shows the changes in  $B_{800}$  and  $\mu_e$  at 1 kHz with  $T_a$  in a constant annealing time for 3.6 ks for the amorphous  $\text{Fe}_{86}\text{Zr}_7\text{B}_6\text{Cu}_1$  alloy, along with the microstructural data obtained by the X-ray diffraction and TEM techniques. Although the  $B_{800}$  is nearly constant ( $\cong 0.7$  T) in the amorphous state, it increases rapidly to 1.5 T at about 800 K by the phase transition from amorphous to bcc phase and remains almost constant up to 973 K. The  $\mu_e$  value also increases drastically by the precipitation of the bcc phase, shows a maximum value of 41000 at 873 K and then decreases rapidly by the transition of bcc to  $\alpha\text{-Fe} + \text{Fe}_3(\text{Zr}, \text{B}) + \text{Fe}_2(\text{Zr}, \text{B})$  phases. In comparison with the previous data (Ref. (9)) on  $B_{800}$  and  $\mu_e$  as a function of  $T_a$ , the changes in  $B_{800}$  and  $\mu_e$  with  $T_a$  and the magnitude of  $B_{800}$  are just the same as those for the melt-spun  $\text{Fe}_{86}\text{Zr}_7\text{B}_6\text{Cu}_1$  ribbon with a cross section of  $0.02 \times 1 \text{ mm}^2$ . However, one can notice that the present magnitude of  $\mu_e$  at  $T_a = 873$  K obtained for the ring-shape sample is much larger than that (17000 at 873 K) for the previous narrower ribbon sample. The  $\mu_e$  value for the narrow ribbon was obtained by a vector impedance analyzer which was different from the present method. The difference in  $\mu_e$  is

too large to be regarded as the difference in the evaluation method. It has previously been reported<sup>(13)</sup> that soft magnetic properties of an amorphous ribbon are strongly dependent on the roughness on the sample surface. That is, the smoother the sample surface the better are the soft magnetic properties. Consequently, the significant increase in  $\mu_e$  for the present wide sample is presumably due to the improvement of smoothness of the sample surface through an optimization of the preparation condition of the wide ribbon sample. The  $\mu_e$  value of 41000 at 1 kHz is comparable to that<sup>(14)(15)</sup> for zero-magnetostrictive Co-Fe-Si-B amorphous alloys having the largest permeability in amorphous alloys.

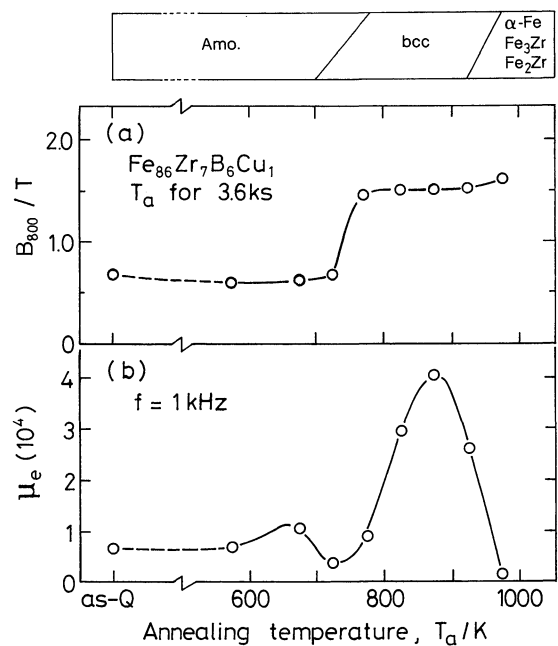


Fig. 4 Changes in the magnetization in a field of 800 kA/m ( $B_{800}$ ) and the permeability at 0.8 A/m ( $\mu_e$ ) as a function of annealing temperature ( $T_a$ ) for an amorphous  $\text{Fe}_{86}\text{Zr}_7\text{B}_6\text{Cu}_1$  alloy. The phase field in as-quenched and annealed states is also shown for reference.

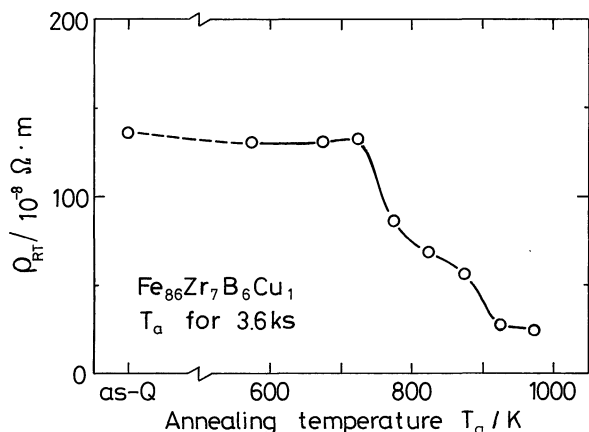


Fig. 5 Change in the electrical resistivity at room temperature ( $\rho_{RT}$ ) as a function of  $T_a$  for an amorphous  $\text{Fe}_{86}\text{Zr}_7\text{B}_6\text{Cu}_1$  alloy.

Figure 5 shows the change in the electrical resistivity at room temperature ( $\rho_{RT}$ ) as a function of  $T_a$  for the amorphous  $\text{Fe}_{86}\text{Zr}_7\text{B}_6\text{Cu}_1$  alloy, along with the data of amorphous  $\text{Fe}_{78}\text{Si}_9\text{B}_{13}$  and bcc  $\text{Fe}-3.5 \text{ mass}\% \text{Si}$  alloys. The  $\rho_{RT}$  value of the Fe-Zr-B-Cu alloy is nearly constant ( $137 \times 10^{-8} \Omega \cdot \text{m}$ ) in an amorphous state in the  $T_a$  range below 723 K. With further increasing  $T_a$ , it decreases rapidly to  $69 \times 10^{-8} \Omega \cdot \text{m}$  in the  $T_a$  range of 723 to 823 K, followed by a gradual decrease to  $56 \times 10^{-8} \Omega \cdot \text{m}$  in the range of 823 to 873 K and then a second rapid decrease to  $26 \times 10^{-8} \Omega \cdot \text{m}$  at temperatures between 873 and 923 K. Thus, the decrease in the  $\rho_{RT}$  value by crystallization occurs through two stages. The first stage is due to the transition of amorphous to bcc phase and the second stage due to bcc to  $\alpha\text{-Fe} + \text{Fe}_3(\text{Zr, B}) + \text{Fe}_2(\text{Zr, B})$  phases. The  $\rho_{RT}$  value was  $132 \times 10^{-8} \Omega \cdot \text{m}$  for the amorphous Fe-Si-B alloy annealed for 3.6 ks at 623 K and  $48 \times 10^{-8} \Omega \cdot \text{m}$  for the heat-treated commercial Fe-Si alloy. Consequently, the  $\rho_{RT}$  value of the bcc Fe-Zr-B-Cu alloy with the highest  $\mu_e$  value is much smaller than that of the Fe-Si-B alloy and slightly larger than that of the Fe-Si alloy.

Figure 6 shows the plots of core loss at 1 T and 50 Hz as a function of  $T_a$  for the amorphous  $\text{Fe}_{86}\text{Zr}_7\text{B}_6\text{Cu}_1$  alloy. The data of amorphous  $\text{Fe}_{78}\text{Si}_9\text{B}_{13}$  and Fe-3.5 mass%Si alloys are also shown for comparison. The core loss of the Fe-Zr-B-Cu alloy changes very sensitively with  $T_a$  and shows a minimum value of 0.066 W/kg at  $T_a = 873 \text{ K}$ . A similar sensitive change in core loss with  $T_a$  is also seen for the amorphous Fe-Si-B alloy and the minimum value is 0.13 W/kg for the amorphous phase annealed at 600 K. It should be noted that the core loss of

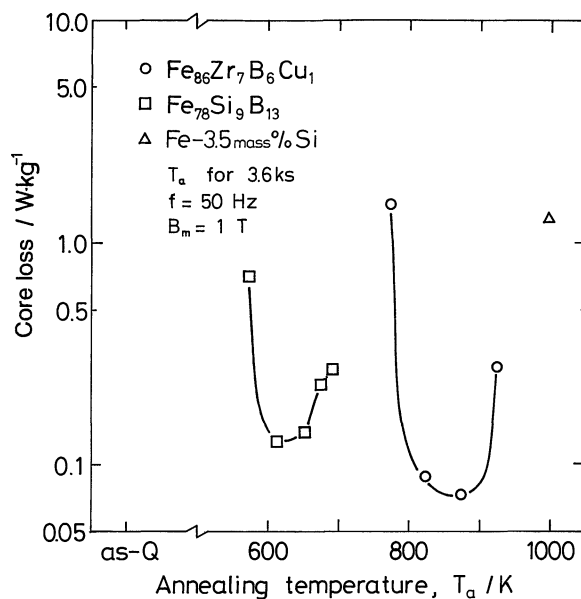


Fig. 6 Change in the core loss as a function of  $T_a$  for an amorphous  $\text{Fe}_{86}\text{Zr}_7\text{B}_6\text{Cu}_1$  alloy. The data of amorphous  $\text{Fe}_{78}\text{Si}_9\text{B}_{13}$  and bcc Fe-3.5 mass%Si alloys are also shown for comparison.

the present bcc Fe-Zr-B-Cu alloy with a grain size of about 10 nm is lower by 47% than that of the amorphous Fe-Si-B alloy and by 95% than that of the Fe-Si alloy. It is thus believed that the present bcc Fe-Zr-B-Cu alloy has the lowest core loss in a number of Fe-based magnetic alloys which include the commercial amorphous Fe-Si-B and bcc Fe-Si alloys. Table 1 summarizes the core loss,  $B_{800}$ ,  $\mu_e$ ,  $H_c$  and  $\rho_{RT}$  values of the bcc  $\text{Fe}_{86}\text{Zr}_7\text{B}_6\text{Cu}_1$  alloy obtained by annealing of the melt-spun amorphous ribbon with a cross section of  $0.021 \times 12.5 \text{ mm}^2$  for 3.6 ks at 873 K. The data for the amorphous  $\text{Fe}_{78}\text{Si}_9\text{B}_{13}$  and bcc Fe-3.5 mass%Si alloys subjected to the optimum heat treatments are also included for comparison. The magnetization value is nearly the same between the Fe-Zr-B-Cu alloy and the Fe-Si-B alloy. However, the  $\mu_e$  of the former alloy is 290% larger and the  $H_c$  is 9% smaller as compared with those for the latter alloy. The better  $\mu_e$  and  $H_c$  values for the Fe-Zr-B-Cu alloy seem to result in the core loss which is 47% smaller than that of the Fe-Si-B alloy. On the other hand, the Fe-Si alloy has the highest magnetization value, but the  $\mu_e$  and  $H_c$  are much worse than the other two alloys, leading to the much larger core loss.

The core loss at 50 Hz of the bcc  $\text{Fe}_{86}\text{Zr}_7\text{B}_6\text{Cu}_1$  alloy produced by annealing the amorphous phase for 3.6 ks at

Table 1 Magnetic properties (core loss,  $B_{800}(B_s)$ ,  $\mu_e$  and  $H_c$ ), electrical resistivity at room temperature ( $\rho_{RT}$ ), structure, optimum annealing temperature ( $T_a$ ) and sample thickness ( $t$ ) of an  $\text{Fe}_{86}\text{Zr}_7\text{B}_6\text{Cu}_1$  alloy and other soft magnetic alloys.

Alloy	$T_a/\text{K}$	Structure	$t/\mu\text{m}$	Core loss*/ $\text{W} \cdot \text{kg}^{-1}$	$B_{800}(B_s)/\text{T}$	$\mu_e^{**}$	$H_c/\text{A} \cdot \text{m}^{-1}$	$\rho_{RT}/10^{-8} \Omega \cdot \text{m}$
$\text{Fe}_{86}\text{Zr}_7\text{B}_6\text{Cu}_1$	873	bcc	21	0.066	1.52	41000	3.2	56
$\text{Fe}_{78}\text{Si}_9\text{B}_{13}$	623	Amorphous	20	0.13	1.58	10400	3.5	132
Fe-3.5 mass%Si	993	bcc	500	1.30	1.97	770	41	48

\* $f=50 \text{ Hz}$ ,  $B_m=1.0 \text{ T}$ , \*\* $f=1 \text{ kHz}$ ,  $H=0.8 \text{ A} \cdot \text{m}^{-1}$ .

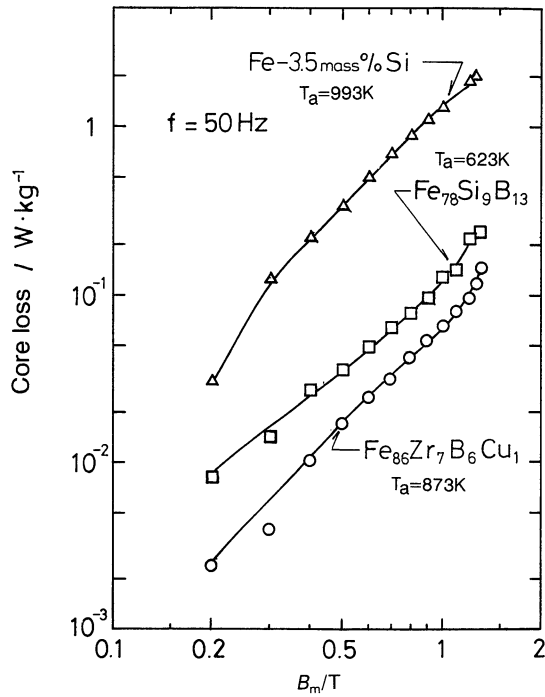


Fig. 7 Relation between core loss and maximum induction field ( $B_m$ ) for a bcc  $\text{Fe}_{86}\text{Zr}_7\text{B}_6\text{Cu}_1$  alloy produced by annealing the melt-spun amorphous phase for 3.6 ks at 873 K. The data of amorphous  $\text{Fe}_{78}\text{Si}_9\text{B}_{13}$  and bcc Fe-3.5 mass%Si alloys are also shown for comparison.

873 K is plotted as a function of maximum induction field ( $B_m$ ) in Fig. 7. The data of the heat-treated amorphous  $\text{Fe}_{78}\text{Si}_9\text{B}_{13}$  and bcc Fe-3.5 mass%Si alloys are also shown for comparison. The core loss of the Fe-Zr-B-Cu alloy increases from 0.0024 to 0.147 W/kg with an increase of  $B_m$  from 0.2 to 1.3 T. Although a similar change of the core loss with  $B_m$  is also seen for the other two alloys, the core loss of the bcc Fe-Zr-B-Cu alloy is the lowest in the entire  $B_m$  range. The rapid increase in the core losses in the  $B_m$  range above about 1.3 T is seen only for the Fe-Zr-B-Cu and Fe-Si-B alloys. This is presumably because the  $B_m$  value approaches the saturation magnetization values of the two alloys. It is thus reconfirmed that the core loss of the bcc Fe-Zr-B-Cu alloy at a commercial frequency of 50 Hz is considerably smaller than those for the bcc Fe-Si alloy and for the amorphous Fe-Si-B alloy. It is well known that the Fe-Si alloy has been used over a decade in various transformers for electrical power distribution and quite recently the Fe-Si-B alloy has been projected to become widely used for the same purpose.

Figure 8 shows the frequency dependence of the  $\mu_e$  value of the bcc  $\text{Fe}_{86}\text{Zr}_7\text{B}_6\text{Cu}_1$  alloy, along with the data of amorphous  $\text{Fe}_{78}\text{Si}_9\text{B}_{13}$  and bcc Fe-3.5 mass%Si alloys. The  $\mu_e$  value remains almost constant ( $\approx 41000$ ) in the frequency range below 3 kHz and decreases gradually with further increasing frequency. However, the  $\mu_e$  value keeps a high level of 9000 even at a high frequency of 100 kHz. As shown in Fig. 8, the  $\mu_e$  values of the bcc Fe-Zr-B-Cu alloy are considerably higher in the entire fre-

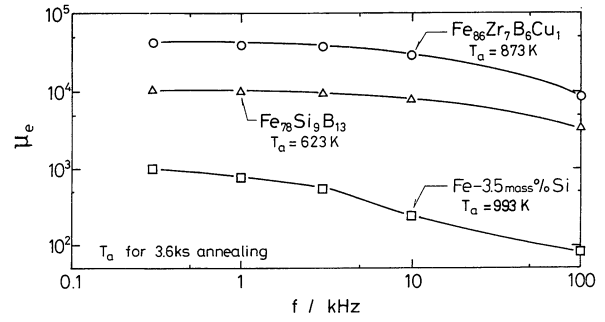


Fig. 8 Change in the  $\mu_e$  value as a function of frequency for a bcc  $\text{Fe}_{86}\text{Zr}_7\text{B}_6\text{Cu}_1$  alloy produced by annealing the melt-spun amorphous phase at 873 K. The data of amorphous  $\text{Fe}_{78}\text{Si}_9\text{B}_{13}$  and bcc Fe-3.5 mass%Si alloys are also shown for comparison.

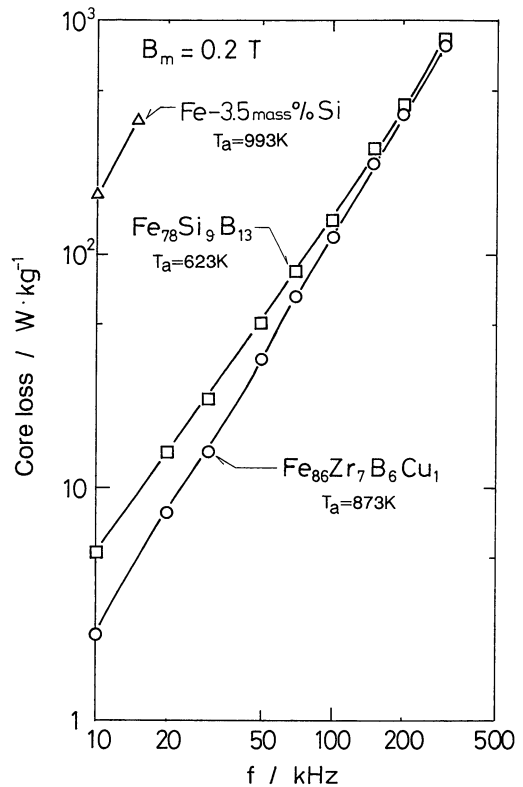


Fig. 9 Relation between core loss and frequency ( $f$ ) for a bcc  $\text{Fe}_{86}\text{Zr}_7\text{B}_6\text{Cu}_1$  alloy produced by annealing the melt-spun amorphous phase for 3.6 ks at 873 K. The data of amorphous  $\text{Fe}_{78}\text{Si}_9\text{B}_{13}$  and bcc Fe-3.5 mass%Si alloy are also shown for comparison.

quency range, as compared with those of the other two alloys. The decrease in the  $\mu_e$  value with increasing frequency is the largest for the bcc Fe-Si alloy, followed by the bcc Fe-Zr-B-Cu alloy and then the amorphous Fe-Si-B alloy. There is a marked tendency that the higher the  $\rho_{RT}$  value (or the smaller the sample thickness) the smaller is the decrease of the  $\mu_e$  value as a function of frequency. The tendency seems to originate from a smaller eddy current loss for the alloy with a higher  $\rho_{RT}$  value or a smaller sample thickness.

The frequency dependence of core loss at  $B_m=0.2$  T was examined for the bcc  $\text{Fe}_{86}\text{Zr}_7\text{B}_6\text{Cu}_1$  alloy exhibiting

the  $\mu_e$  value of 41000 at 1 kHz, in comparison with the data of the amorphous  $\text{Fe}_{78}\text{Si}_9\text{B}_{13}$  and bcc Fe-3.5 mass%Si alloys subjected to the optimum heat treatments. The dependence is important to evaluate the possibility of practical use as a core material in high-frequency transformers such as switching power supply and inverter. As shown in Fig. 9, the core loss at 10 kHz of the Fe-Zr-B-Cu alloy is 127% lower than that of the Fe-Si-B alloy, but the difference decreases to 6% with an increase of frequency to 300 kHz. Considering that the core loss is inversely proportional to  $\rho_{\text{RT}}$  and in direct proportion to the square of frequency, the decrease of the difference is due to the much larger  $\rho_{\text{RT}}$  for the amorphous Fe-Si-B alloy. In addition, one can notice that the Fe-Si alloy has much larger core losses in the entire frequency range as compared with those of the other two alloys. It is therefore expected that the present bcc Fe-Zr-B-Cu alloy may also be used as a core material in high frequency transformers in which Fe-Si-B amorphous alloys are presently being used<sup>(16)</sup>.

#### IV. Summary

The core loss of a bcc  $\text{Fe}_{86}\text{Zr}_7\text{B}_6\text{Cu}_1$  alloy with a grain size of about 10 nm was examined in relation to other magnetic and electrical properties of  $\mu_e$ ,  $B_{800}$  and  $\rho_{\text{RT}}$ . The alloy was chosen because of its high permeability and high saturation magnetization. The results obtained are summarized as follows.

(1) The bcc Fe-Zr-B-Cu alloy produced by annealing the melt-spun amorphous phase for 3.6 ks at 873 K exhibits high  $B_{800}$  and  $\mu_e$  values of 1.52 T and 41000 at 1 kHz, respectively. The  $\mu_e$  value is almost comparable to that for zero-magnetostrictive Co-Fe-Si-B amorphous alloys.

(2) The electrical resistivity at room temperature ( $\rho_{\text{RT}}$ ) decreases first from  $137 \times 10^{-8}$  to  $69 \times 10^{-8} \Omega \cdot \text{m}$  by the transition of amorphous to bcc phase at about 750 K. The following decrease to  $26 \times 10^{-8} \Omega \cdot \text{m}$  occurs by the subsequent transition of bcc to  $\alpha\text{-Fe} + \text{Fe}_3(\text{Zr}, \text{B}) + \text{Fe}_2(\text{Zr}, \text{B})$  phases at about 900 K.

(3) The core loss at  $B_m = 1$  T and 50 Hz for the bcc Fe-Zr-B-Cu alloy exhibits a minimum value of 0.066 W/kg at  $T_a = 873$  K. The minimum value is smaller by 49% than that for the amorphous  $\text{Fe}_{78}\text{Si}_9\text{B}_{13}$  alloy and by 95% than that for the bcc Fe-3.5 mass%Si alloy.

(4) The core losses at  $B_m = 0.2$  T for the bcc  $\text{Fe}_{86}\text{Zr}_7\text{B}_6\text{Cu}_1$  alloy increase from 2.33 to 780 W/kg with an increase of frequency from 10 to 300 kHz. However, their values are superior to those of the amorphous  $\text{Fe}_{78}\text{Si}_9\text{B}_{13}$  and bcc Fe-3.5 mass%Si alloys in the entire frequency range. The low core losses combined with high  $B_{800}$  and  $\mu_e$  values lead to an expectation that the core materials made from amorphous Fe-Si-B and bcc Fe-Si alloys in various types of transformers could be at least partly replaced by the newly developed bcc Fe-Zr-B-Cu alloy with nanoscale grain size.

#### Acknowledgment

The authors acknowledge helpful discussions with Prof. K. V. Rao of Department of Condensed Matter Physics, The Royal Institute of Technology in Sweden on several points in the paper.

#### REFERENCES

- (1) H. Fujimori: *Materials Science of Amorphous Metals*, ed. by T. Masumoto, Ohmu Pub. Co., (1982), p. 97.
- (2) R. Hasegawa, G. E. Fish and V. R. V. Rammanan: *Proc. 4th Int. Conf. on Rapidly Quenched Metals*, ed. by T. Masumoto and K. Suzuki, Japan Inst. Metals, Sendai (1981), p. 929.
- (3) Y. Ogata, Y. Sawada and T. Miyazaki: *Proc. 4th Int. Conf. on Rapidly Quenched Metals*, ed. by T. Masumoto and K. Suzuki, Japan Inst. Metals, Sendai (1981), p. 953.
- (4) Y. Yoshizawa, S. Oguma and K. Yamauchi: *J. Appl. Phys.*, **64** (1988), 6044.
- (5) N. Hasegawa and M. Saito: *J. Magn. Soc. Japan*, **14** (1990), 313.
- (6) A. Inoue, K. Kobayashi, M. Nose and T. Masumoto: *J. de Phys.*, C-8, **41** (1980), 831.
- (7) S. Ohnuma, M. Nose, K. Shirakawa and T. Masumoto: *Sci. Rep. Res. Inst. Tohoku Univ.*, **A29** (1981), 254.
- (8) K. Suzuki, N. Kataoka, A. Inoue, A. Makino and T. Masumoto: *Mater. Trans.*, JIM, **31** (1990), 743.
- (9) K. Suzuki, A. Makino, N. Kataoka, A. Inoue and T. Masumoto: *Mater. Trans.*, JIM, **32** (1991), 93.
- (10) W. B. Pearson: *A Handbook of Lattice Spacings and Structures of Metals and Alloys*, Pergamon Press, Oxford (1964), p. 625.
- (11) N. Kataoka, K. Suzuki, A. Inoue and T. Masumoto: *J. Mater. Sci.*, in press.
- (12) M. Komuro: Master Thesis, Tohoku University (1984).
- (13) M. Matsuura, M. Kikuchi, M. Yagi and K. Suzuki: *Jpn. J. Appl. Phys.*, **19** (1980), 1781.
- (14) H. Fujimori, M. Kikuchi, Y. Obi and T. Masumoto: *Sci. Rep. Res. Inst. Tohoku Univ.*, **A-26** (1976), 36.
- (15) Y. Makino, K. Aso, S. Uedaira, M. Hayakawa, Y. Ochiai and H. Hotai: *J. Appl. Phys.*, **52** (1981), 2477.
- (16) M. Mitera, H. Fujimori and T. Masumoto: *Proc. 4th Int. Conf. on Rapidly Quenched Metals*, ed. by T. Masumoto and K. Suzuki, Japan Inst. Metals, Sendai (1981), p. 1011.